and 25 °C, and a value exceeding 100 M^{-1} does not seem to be reported so far. Further, the association constants obtained for I–IV increase as the acidity of the complexes increases, and a good linear correlation between log K and pK_a may be observed in Figure 7. A linear regression analysis for the malonate and sulfate systems yields 0.98 and 0.90 as the correlation coefficients, but these figures should not be taken too literally because of rather large uncertainties in pK_a values and some K values. Thus, log K can also be correlated with pK_{a1} alone rather well. Even with these reservations, the correlation seems satisfactory. With the CD changes in Figure 5 and the correlation in Figure 7 taken together, it appears reasonable to conclude that the malonate and sulfate anions approach the complex cations from the D_3 equatorial direction and hydrogen bond, via two oxygen atoms of the anions, to two NH hydrogens of the cations, and the stability of the ion pairs is governed by this double hydrogen bonding.

It seems pertinent to consider here the factors that may affect the value of the outer-sphere association constant in aqueous solution. Here, we will confine our discussion to such complexes that do not contain very hydrophobic ligands, as typified by 1,10-phenanthroline or 2,2′-bipyridine. For complexes with an overall charge of 1+ or 2+, we have pointed out that the dominant factor is the size of the interacting ions; as the ions get larger[16] and hence assume more and more the character of water-structure breaker,[17] the association constant increases. Here, it was noted that it is the crystallographic volume, not the hydrodynamic volume, of the ions that governs the association constant. This appears to be suggestive of contact ion pairs. For complexes with an overall charge of 3+, it is certain that interionic electrostatic force usually contributes significantly. This will be readily appreciated if we note a general trend in association constant that tripositive complex cations exhibit much larger association constant for most simple anions like Cl^-, Br^-, NO_3^-, SO_4^{2-}, or $S_2O_3^{2-}$ than monopositive and dipositive complex cations.[2c] However, a cursory examination of previous results reveals immediately that the electrostatic force alone may not explain the variation of K values. For example, the K values of $[Co(en)_3]^{3+}$ for *o*- and *p*-phthalate dianions are repoted to be about 65 and 2.8 M^{-1}, respectively, at μ = 0.1 ($NaClO_4$) and 25 °C.[1j] Likewise, large differences in K values of perhaps a similar nature can also be found for $[Co(en)_3]^{3+}$···maleate/fumarate and $[Co(en)_3]^{3+}$···*cis*-1,2-/1,4-cyclohexanedicarboxylates (48 vs. 3.5 M^{-1} and 70 vs. 8.5 M^{-1}, respectively, under the same condition as above),[1j,14] despite the same 3+/2− combination. Since such large differences in K values may not be accommodated by a simple electrostatic consideration[18] and only those anions that can allow both carboxyl groups to take part in bonding to NH hydrogens of the cation simultaneously exhibited large K values, the importance of hydrogen bonding has been stressed.[14] Therefore, it may be inferred that both electrostatic force and hydrogen bonding contribute significantly for tripositive complexes. The relative importance of the two effects has not always been assessed. We believe that the present result provides an unequivocal example where ion pairing is controlled by (double) hydrogen bonding.

The results presented in Figure 7 might appear at first sight to suggest that the K values of ordinary complexes with $pK_a > 14$ are dominated by factors other than hydrogen bonding; hydrogen bonding plays a minor role in $[Co(en)_3]^{3+}$. Though double hydrogen bonding with $[Co(en)_3]^{3+}$ as depicted in Figure 6 is equally plausible structurally as for the present complexes, a completely different mode of association has been proposed for $[Co(en)_3]^{3+}$.[1c,d,2a] In the ion pair $[Co(en)_3]^{3+}$···SO_4^{2-}, for example, the sulfate ion has been assumed to approach the cation along the cation's C_3 axis and hydrogen bond, through three oxygen atoms, to three NH hydrogens of the cation that are oriented in the C_3 direction. For the dicarboxylate anions cited above, a similar C_3 access has been postulated. Therefore, it may be inappropriate to discuss $[Co(en)_3]^{3+}$ and the present complexes on the same basis.

From Figure 7 and Table I, it is seen that the association constant with malonate is rather similar to that with sulfate for all the complexes investigated in this work. This similarity in K values is puzzling for the present systems, where the dominant factor in K is most probably the hydrogen bonding; in hydrogen-bonded systems, the K values are expected to depend not only on the acidity of the complexes but also on the basicity of the anion.[15] This reasoning leads us to expect that the sulfate ion should have smaller K values than the malonate ion, because the former is less basic than the latter. Though the difference in K values is not large, especially for IV, the results in Table I do not appear to support this expectation. In this contrast, it may be worhwhile to point out that such an expectation is not fulfilled also for systems like $[Co(en)_3]^{3+}$···dicarboxylate dianions, where hydrogen bonding is considered to be the dominant contributor.

Acknowledgment. The authors are grateful to Prof. A. M. Sargeson for informing them of acidity data of related complexes prior to publication and to K. Honda for experimental assistance.

(16) Pethybridge, A. D.; Spiers, D. J. *J. Chem. Soc., Faraday Trans. 1*, **1976**, *72*, 64–72, 73–78.
(17) Yoneda, H.; Wakida, S.; Nakazawa, H.; Sakaguchi, U. *Bull. Chem. Soc. Jpn.* **1982**, *55*, 1073–1076.
(18) See, e.g.: Yokoyama, H.; Yamatera, H. *Bull. Chem. Soc., Jpn.* **1975**, *48*, 1770–1776.

Contribution from AT&T Bell Laboratories,
Murray Hill, New Jersey 07974

Molecular Orbital Justification of Topological Electron-Counting Theory

BOON K. TEO

Received June 26, 1984

It is shown that the rules for determining the parameter X of the topological electron-counting (TEC) theory or its generalized version can be justified within the framework of molecular orbital theory. The parameter X can be interpreted as the number of "missing" antibonding cluster orbitals, or more precisely $X = E - A$, where E is the number of edges and A is the number of antibonding cluster orbitals. It is also shown that the number of *bonding* cluster orbitals corresponds to the number of skeletal electron pairs in the context of the widely used skeletal electron pair (SEP) theory. Consequently, both rules can be derived from molecular orbital calculations and vice versa. Qualitative correlation and interaction diagrams are constructed for the conversion of prisms to antiprisms, pyramids to bipyramids, and prisms to bicapped prisms. Multiple X values, and hence multiple electron counts, for certain polyhedral clusters are also justified and illustrated with examples.

Introduction

Recently we developed a new topological electron-counting (TEC) theory for polyhedral metal clusters based on Euler's theorem and the effective atomic number (EAN) rule for transition metals.[1] This theory was subsequently generalized to include polyhedral clusters containing both main-group and transition-metal elements.[2] This simple electron-counting rule can be used

(1) (a) Teo, B. K. *Inorg. Chem.* **1984**, *23*, 1251. (b) Teo, B. K.; Longoni, G.; Chung, F. R. K. *Inorg. Chem.* **1984**, *23*, 1257.

0020-1669/85/1324-1627$01.50/0

to correlate the known structures as well as to predict the yet unknown geometries of a wide range of polyhedral clusters of varying nuclearity, including boranes, carbanes, carboranes, metallaboranes, metallacarboranes, and main-group and/or transition-metal clusters, etc.[3-5] It also provides a better understanding of the interrelations and/or transformations of various cluster geometries.

Central to the TEC theory is the evaluation of the "adjustment" parameter X, which, until now, has been qualitatively interpreted as either (1) the number of electron pairs "in excess" of the EAN and/or octet rule or (2) the number of "false" bonds (assuming that each polyhedral edge corresponds to a two-center two-electron bond). A more quantitative interpretation of the parameter X is that it corresponds to the number of "missing" *antibonding cluster orbitals* (when compared with the number of *edges*, viz., nearest neighbor contacts). In this latter context, one should be able to justify the rules for determining the parameter X within the framework of molecular orbital theory. In this paper, we wish to show that the rules for determining the parameter X can easily be derived from molecular orbital calculations. This quantitative measure of the parameter X provides not only an independent verification of the validity of the rules but also a new way of calculating the parameter X for polyhedra for which the applications of the rules are not straightforward.

In a related work,[2] we also demonstrated that the number of *skeletal electron pairs*, in the context of skeletal electron pair (SEP) theory,[6] can be calculated from the parameter X. The TEC method therefore provides an alternative and sometimes complementary means of evaluating the number of skeletal electron pairs for polyhedral clusters.[7] In this paper, it will be shown that the number of skeletal electron pairs can be given by the number of *bonding cluster orbitals* and, therefore, is indirectly related to the parameter X, which is equal to the number of "missing" *antibonding cluster orbitals*.

A useful utility of the TEC theory is that it allows us to evaluate the number of bonding and antibonding cluster orbitals from the parameter X (which can be determined readily from the rules) without extensive molecular orbital calculations. However, it should be emphasized that, in contrast to molecular orbital calculations, and as with any other electron-counting rules, the method provides no detailed information concerning the symmetry and/or energetics of orbital interactions (except the number of such interactions) within the cluster.

Also discussed are the correlation and interaction diagrams for the conversion of prisms to antiprisms, pyramids to bipyramids, and prisms to bicapped prisms.

Table I. Rules for X

		highest symmetry axis				
rule	polyhedron	3	4	5	6	7
1	3-connected	0	0	0	0	0
2	capping[a]	0	1	2	3	4
3	pyramid	0	0	0	0	0
4	bipyramid[b]	0^c, 2^d	$1^{c,d}$, 3^d	$2^{c,d}$	$3^{c,d}$	$4^{c,d}$
5	antiprism[e]	1	3, 1	3	3	3
6	vertex- or edge-sharing	$X = S$ (no. of shared vertices or edges)				
	face-sharing	$X = -H$ (no. of hidden edges, if any)				
7	perturbation	$\Delta X \leq \Delta F + Y$				

[a] Capping an n-gonal face changes X by $n - 3$. [b] The X value for bipyramids can be determined either by capping the corresponding pyramids or by counting the number of *antibonding* Hückel orbitals. [c] X value determined by capping. [d] X value determined by counting the antibonding Hückel orbitals. [e] The X value for antiprisms can be determined by counting the *bonding* Hückel orbitals.

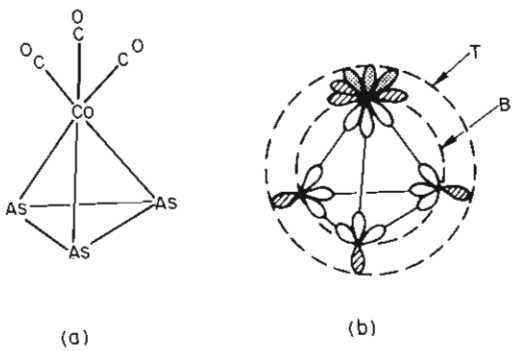

Figure 1. (a) Structure of $As_3Co(CO)_3$, a tetrahedral cluster. (b) Pictorial representation of the topological electron pairs, T (outer circle), and the skeletal electron pairs, B (inner circle). See text for more details.

Multiple X values (and hence multiple electron counts) for certain polyhedral clusters are also justified within the framework of molecular orbital theory and illustrated with some representative examples.

Topological Electron-Counting Theory

For a polyhedron with V vertices, F faces, and E edges, Euler's theorem states that

$$E = V + F - 2 \tag{1}$$

Let

$$V = V_n + V_m \tag{2}$$

where V_n and V_m are the numbers of vertex atoms having the tendency to conform to the 8- and 18-electron noble-gas configuration (viz., the octet and the effective atomic number rules), respectively. Assuming that each edge can be considered as a two-center electron-paired bond, the total electron count is

$$N = 8V_n + 18V_m - 2E \tag{3}$$

Note that N includes all valence electrons from the vertex atoms as well as electrons donated by the ligands or the encapsulated atoms to the cluster. The total number of *topological electron pairs* is

$$T = N/2 = 4V_n + 9V_m - E \tag{4}$$

In general, T corresponds to Lauher's cluster valence molecular orbitals (CVMO).[8] Substituting eq 1 and 2 into eq 4 gives

$$T = 3V_n + 8V_m - F + 2 \tag{5}$$

However, for a delocalized system, not all edges of the polyhedron can be considered as two-center two-electron bonds. This implies that a correction factor X must be added to eq 5:

(2) Teo, B. K., submitted for publication.
(3) For reviews on boranes, carboranes, metallaboranes, and metallacarboranes, see, e.g.: (a) Lipscomb, W. N. "Boron Hydrides"; W. B. Benjamin: New York, 1963. (b) Muetterties, E. L., Ed. "Boron Hydride Chemistry"; Academic Press: New York, 1975. (c) Muetterties, E. L.; Knoth, W. H. "Polyhedral Boranes"; Marcel Dekker: New York, 1968. (d) Rudolph, R. W. *Acc. Chem. Res.* **1976**, *9*, 446. (e) Grimes, R. N. "Carboranes"; Academic Press: New York, 1970. (f) Grimes, R. N., Ed. "Metal Interactions with Boron Clusters"; Plenum Press: New York, 1982. (g) O'Neill, M. E.; Wade, K. (Chapter 1); Onak, T. (Chapter 5.4); Grimes, R. N. (Chapter 5.5). In "Comprehensive Organometallic Chemistry"; Wilkinson, G., Stone, F. G. A., Abel, E. W., Eds.; Pergamon Press: New York, 1982; Vol. 1.
(4) For reviews on main-group clusters, see, e.g.: (a) Corbett, J. D. *Prog. Inorg. Chem.* **1976**, *21*, 129. (b) Gillespie, R. J. *Chem. Soc. Rev.* **1979**, *8*, 315.
(5) For reviews on transition metal clusters, see, e.g.: (a) Chini, P. *Gazz. Chim. Ital.* **1979**, *109*, 225. (b) Chini, P. *J. Organomet. Chem.* **1980**, *200*, 37. (c) Chini, P.; Longoni, G.; Albano, V. G. *Adv. Organomet. Chem.* **1976**, *14*, 285. (d) "Transition Metal Clusters"; Johnson, B. F. G., Ed., Wiley-Interscience: Chichester, England, 1980. (e) Benfield, R. E.; Johnson, B. F. G. *Top. Stereochem.* **1981**, *12*, 253.
(6) (a) Williams, R. E. *Inorg. Chem.* **1971**, *10*, 210. (b) Rudolph, R.; Pretzer, W. R. *Inorg. Chem.* **1972**, *11*, 1974. (c) Wade, K. *J. Chem. Soc., Chem. Commun.* **1971**, 792; *Inorg. Nucl. Chem. Lett.* **1972**, *8*, 559, 563. (d) Wade, K. *Chem. Br.* **1975**, *11*, 177. (e) Wade, K. *Adv. Inorg. Chem. Radiochem.* **1976**, *18*, 1. (f) Mingos, D. M. P. *Nature (London), Phys. Sci.* **1972**, *236*, 99. (g) Mason, R.; Thomas, K. M.; Mingos, D. M. P. *J. Am. Chem. Soc.* **1973**, *95*, 3802.
(7) Teo, B. K. *Inorg. Chem.* **1985**, *24*, 115.
(8) (a) Lauher, J. W. *J. Am. Chem. Soc.* **1978**, *100*, 5305. (b) Lauher, J. W. *J. Am. Chem. Soc.* **1979**, *101*, 2604. (c) Lauher, J. W. *J. Organomet. Chem.* **1981**, *213*, 25.

$$T = N/2 = 3V_n + 8V_m - F + 2 + X \quad (6)$$

where X is the number of "extra" electron pairs "in excess" of the effective atomic number (EAN) rule. The rules for estimating the parameter X are summarized in Table I. Note that eq 6 is a generalized version of the TEC rule.[1,2]

We shall illustrate the utility of the TEC theory with an example, $As_3Co(CO)_3$,[9] shown in Figure 1a. With $V_n = 3$, $V_m = 1$, $F = 4$, and $X = 0$ (rule 1), eq 6 predicts $T = 3 \times 3 + 8 \times 1 - 4 + 2 + 0 = 15$, or a total of $N = 2 \times 15 = 30$ electrons. This is in agreement with the observed electron count of 3×5 (As) $+ 1 \times 9$ (Co) $+ 3 \times 2$ (CO) $= 30$. Note that the Co atom contributes nine atomic orbitals and nine electrons while each As atom contributes four atomic orbitals and five electrons to cluster bonding. The disposition of the fifteen topological electron pairs, T (outer circle), is shown pictorially in Figure 1b: three bonding electron pairs donated by the three carbonyls (dotted), six lone pairs (crossed), three from the Co atom and one from each of the three As atoms, and six bonding electron pairs that occupy the bonding combinations of the twelve cluster orbitals (open), three from each vertex atom.

If the electron pairs "exo" to the cluster (cf. dotted or crossed orbitals in Figure 1b) are removed, one obtains a quantity B (cf. inner circle, Figure 1b):

$$B = T - (V_n + 6V_m) \quad (7)$$

Combining eq 6 and 7 gives[2]

$$B = 2V - F + 2 + X \quad (8)$$

Parameter B can be interpreted as the number of *bonding cluster* orbitals or electron pairs. As it turns out, parameter B corresponds to the number of *skeletal electron pairs* in the context of the skeletal electron pair (SEP) theory.[6] It is interesting to note that B depends on the total number of vertices, V, regardless of its makeup (V_n and V_m).

It is apparent that eq 8 allows a direct comparison between the TEC and the SEP rules. As we shall see in the following sections, both theories can be derived from molecular orbital calculations.

Antibonding vs. Bonding Cluster Orbitals

In this section, we shall provide a firm theoretical footing for the adjustment parameter X. We shall also show how it is related to the number of *antibonding* (A) and *bonding* (B) cluster orbitals.

In the context of molecular orbital theory, the parameter X can be interpreted as the number of "missing" antibonding cluster orbitals (assuming that each polyhedral edge corresponds to a single-bond distance):

$$X = E - A \quad (9)$$

where A is the number of *antibonding cluster orbitals*. If it is assumed that each vertex atom contributes mainly three orbitals for cluster bonding,[10] then there are a total of $3V$ cluster orbitals such that

$$A + B = 3V \quad (10)$$

Chart I

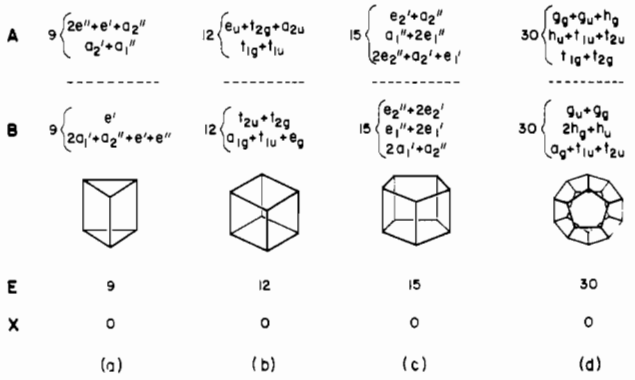

Chart II

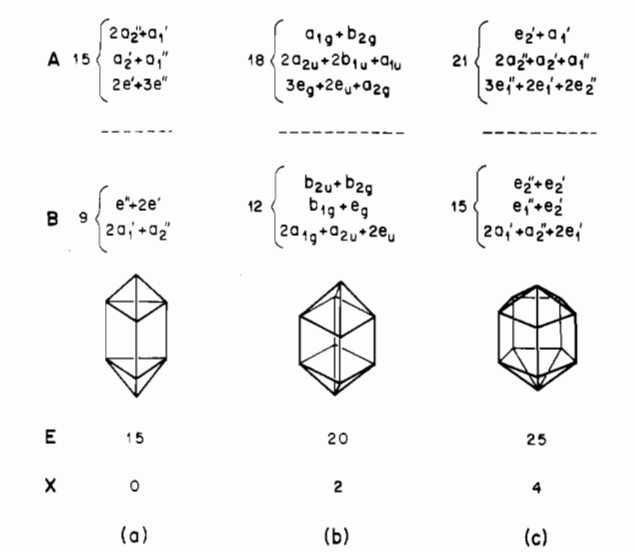

where B is the number of *bonding cluster orbitals*. From molecular orbital calculations, one obtains quantities A and B, and from eq 9, the parameter X can readily be calculated as we shall see in the next section.

Conversely, one can predict the number of the antibonding (A) and the bonding (B) cluster orbitals from the parameter X via the rules tabulated in Table I. Combining eq 1 and 9, we obtain

$$A = E - X = V + F - 2 - X \quad (11)$$

Combining eq 10 and 11, we have

$$B = 3V - A = 2V - F + 2 + X \quad (12)$$

Note that we have rederived eq 8 in the context of molecular orbital theory.

It is obvious from the foregoing discussion that any given polyhedron can be characterized by one of the three parameters, X, A, or B. These parameters are interchangeable via eq 9–12. The electron-counting problem therefore reduces to determining one of these three parameters. As it turns out, the TEC theory provides a measure of X, the SEP rule is related to the parameter B, and, as we shall see in the next section, all three parameters X, A, and B, can readily be obtained from MO calculations.

Derivation of X from Molecular Orbital Calculations

Much of the information needed to derive the adjustment parameter X can be found in the extensive extended Hückel molecular orbital (EHMO) calculations for polyhedral boron hydride clusters ($B_nH_n^{2-}$) by Hoffmann and Lipscomb.[11] In this landmark paper, published in 1962, Hoffmann and Lipscomb examined

(9) Foust, A. S.; Foster, M. S.; Dahl, L. F. *J. Am. Chem. Soc.* **1969**, *91*, 5631.

(10) A crude approximation is to consider the *three* orbitals contributed by each vertex atom for cluster bonding as *hybrid* orbitals pointing inward (away from the exo ligands). A better description can be obtained via the *isolobal* concept. For example, the octahedral cluster $H_2Ru_6(CO)_{18}$ is equivalent to *closo*-$B_6H_6^{2-}$ since each $Ru(CO)_3$ unit with d^5sp^3 hybridization is *isolobal* with a BH unit (with sp^3 hybridization) in that each vertex atom contributes two electrons and three orbitals for cluster bonding (assuming each ruthenium has three essentially nonbonding electron pairs). Hence, both clusters require seven skeletal electron pairs ($B = 7$), as is indeed observed. By the same rationale, the square-pyramidal cluster $Ru_5(CO)_{15}C$ is equivalent to *nido*-B_5H_9 with seven skeletal electron pairs. For more details on the *isolobal* concept, see, for example: (a) Elian, M.; Chen, M. M. L.; Mingos, D. M. P.; Hoffmann, R. *Inorg. Chem.* **1976**, *15*, 1148. (b) Hoffmann, R. *Science (Washington, DC)* **1981**, *211*, 995. (c) Schilling, B. E. R.; Hoffmann, R. *J. Am. Chem. Soc.* **1979**, *101*, 3456. (d) Hoffmann, R.; Schilling, B. E. R.; Bau, R.; Kaesz, H. D.; Mingos, D. M. P. *J. Am. Chem. Soc.* **1978**, *100*, 6088. (e) Halpern, J. *Discuss. Faraday Soc.* **1968**, *46*, 7. (f) Ellis, J. E. *J. Chem. Educ.* **1976**, *53*, 2. (g) Stone, F. G. A. *Acc. Chem. Res.* **1981**, *14*, 318. (h) Mingos, D. M. P. *Trans. Am. Crystallogr. Assoc.* **1980**, *16*, 17. (i) Albright, T. A. *Ibid.* **1980**, *16*, 35.

(11) Hoffmann, R.; Lipscomb, W. N. *J. Chem. Phys.* **1962**, *36*, 2179.

Chart III

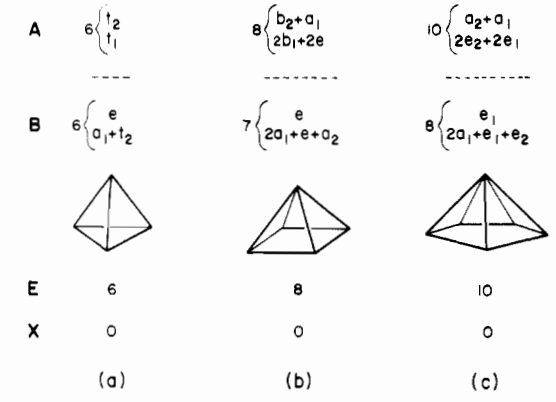

Chart IV

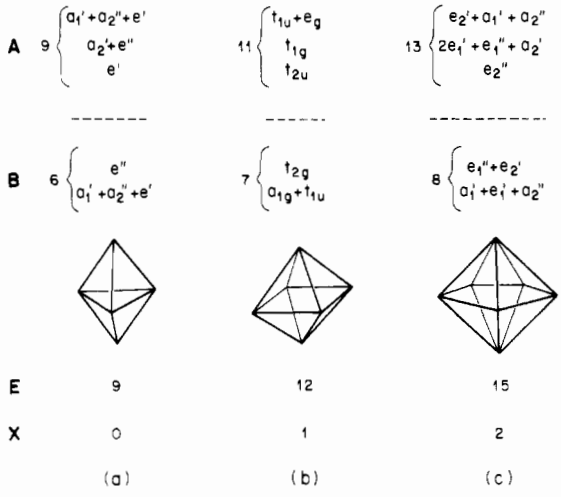

various factorization schemes and found that the B–H bonds, exo to the polyhedron, can be dropped without seriously affecting the energetics of the ground state. The orbitals that were "factored out" are the hydrogen 1s orbital and the boron sp^3 hydrid orbital directed outward. Each boron atom therefore has three sp^3 hybrid orbitals, directed inward, responsible for cluster bonding. This factorization scheme is called "3*N*" in Hoffmann and Lipscomb's paper. We shall use their "3*N*" results in the following derivation of *X* for all polyhedra discussed here except those for the pentagonal prism and pentagonal dodecahedron, which were taken from Honegger et al.[12] and Schulman et al.,[13] respectively. The energy level diagrams for trigonal and pentagonal prisms (Chart Ia,c) as well as those for tetragonal and pentagonal antiprisms (Chart Vb,c) were obtained by removing the symmetry orbitals of the two capping atoms from the corresponding bicapped polyhedra.

It is important to note that Hoffmann and Lipscomb's finding that "3*N*" calculations are quite good approximations for ground-state electronic configurations provides a strong theoretical basis for the assumption that each vertex atom contributes basically three orbitals for cluster interactions. It is also apparent that *B* and *T* in this paper correspond to the number of bonding orbitals from the "3*N*" and "5*N*" calculations in Hoffmann and Lipscomb's paper[11] (note: $B = 2V - F + 2 + X$ and $T = 3V - F + 2 + X$ for main-group clusters).

The energy levels, grouped into bonding and antibonding bands separated by the energy zero (dashed line) for some representative polyhedral clusters, are shown in Charts I–V and VII. Examples can be found in ref 1 and 2. In some cases, the nearly nonbonding

Chart V

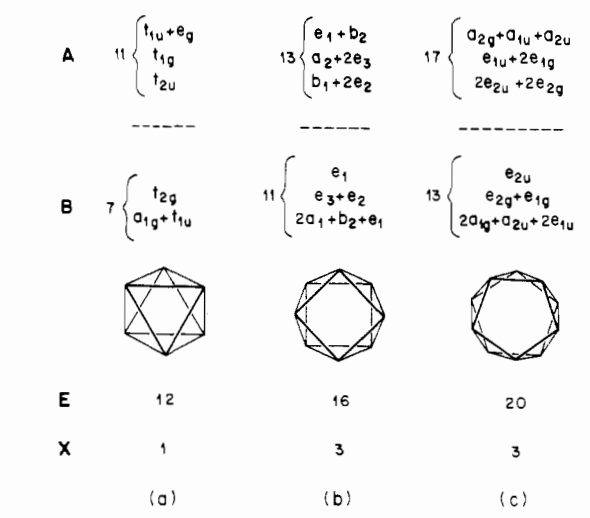

Chart VI

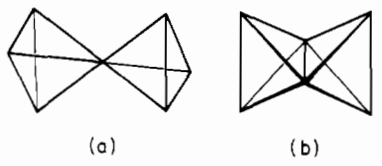

Chart VII

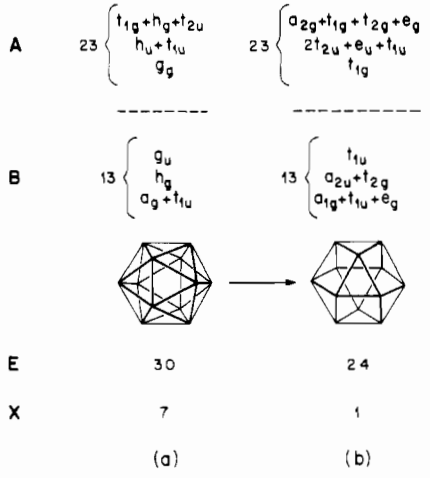

orbitals, either bonding or antibonding, are singled out and grouped separately. The total number of bonding (*B*) and antibonding (*A*) cluster orbitals are also given to the left of each band. The total of $A + B$ must be equal to $3V$ (cf. eq 10). If the number of edges, *E*, is known, the parameter $X = E - A$ (eq 9) can readily be calculated as shown in Charts I–V and VII (cf. Table I).

Rule 1. For 3-connected polyhedra such as the trigonal prism, cube (or tetragonal prism), or pentagonal prism, $A = B = E$, it follows that $X = E - A = 0$ (cf. Chart Ia–c). For example, the cube has 12 bonding ($a_{1g} + t_{1u} + e_g + t_{2u} + t_{2g}$) and 12 antibonding ($t_{1g} + t_{1u} + e_u + t_{2g} + a_{2u}$) cluster orbitals; hence $B = A = 12$. With 12 edges ($E = 12$), $X = E - A = 12 - 12 = 0$. Also included in Chart I is the pentagonal dodecahedron (Chart Id).[13] With $A = 30$, $B = 30$, and $E = 30$, $X = E - A = 30 - 30 = 0$ is readily deduced. It is concluded that $X = 0$ for 3-connected polyhedra.

Rule 2. In ref 11, the energy levels for the bicapped trigonal, tetragonal, and pentagonal prisms were calculated. As shown in Chart IIa, there are 9 bonding (*B*) and 15 antibonding (*A*) cluster orbitals for the D_{3h} bicapped trigonal prism. With 15 edges (*E*), it follows that $X = E - A = 15 - 15 = 0$. Since the trigonal prism has $X = 0$, it is obvious that capping a triangular face gives rise to $X = 0/2 = 0$. For the D_{4h} bicapped cube, Chart IIb shows that $B = 12$ and $A = 18$. With $E = 20$, we deduce $X = E - A = 20$

(12) Honegger, E.; Eaton, P. E.; Shankar, B. K. R.; Heilbronner, E. *Helv. Chim. Acta.* **1982**, *65*, 1982.
(13) Schulman, J. M.; Venanzi, T.; Disch, R. L. *J. Am. Chem. Soc.* **1975**, *97*, 5335.

$- 18 = 2$. Since the cube has $X = 0$, it follows that capping a square face will contribute $X = 2/2 = 1$. For the D_{5h} bicapped pentagonal prism, Chart IIc shows that $B = 15$ and $A = 21$. With $E = 25$, $X = 25 - 21 = 4$. Once again, since the parent polyhedron, the pentagonal prism, has $X = 0$, it follows that capping a pentagonal face will give rise to $X = 4/2 = 2$. It is concluded that X increases by $n - 3$ for capping an n-gonal face.

Rule 3. The energy levels and the derivation of the X values for the pyramids are shown in Chart III. The tetrahedron (or trigonal pyramid) has $B = 6$ bonding ($a_1 + t_2 + e$) and $A = 6$ antibonding ($t_1 + t_2$) cluster orbitals; with $E = 6$ edges, $X = E - A = 6 - 6 = 0$ is obtained. For the tetragonal pyramid, with $B = 7$, $A = 8$, and $E = 8$, $X = 8 - 8 = 0$. And, for the pentagonal pyramid, with $B = 8$, $A = 10$, and $E = 10$, $X = 10 - 10 = 0$. It is therefore concluded that $X = 0$ for pyramids.

Rule 4. The energy levels and the X values for bipyramids are depicted in Chart IV. The trigonal bipyramid (Chart IVa) has $B = 6$ bonding ($a_1' + a_2'' + e' + e''$) and $A = 9$ antibonding ($e' + a_2' + e'' + a_1' + a_2'' + e'$) cluster orbitals and $E = 9$ edges; it follows that $X = E - A = 9 - 9 = 0$. The octahedron (Chart IVb) has $B = 7$ (bonding ($a_{1g} + t_{1u} + t_{2g}$) and $A = 11$ antibonding ($t_{2u} + t_{1g} + t_{1u} + e_g$) orbitals and $E = 12$ edges; it follows that $X = E - A = 12 - 11 = 1$. Finally, the pentagonal bipyramid (Chart IVc) has $B = 8$, $A = 13$, and $E = 15$; it follows that $X = 15 - 13 = 2$. The additional X value for trigonal ($X = 2$) and tetragonal ($X = 3$) bipyramids will be discussed in a later section (under the heading Multiple X Values).

Rule 5. The antiprisms are depicted in Chart V. The undistorted trigonal antiprism or the octahedron (Chart Va) has been discussed under rule 4. The energy levels for the tetragonal antiprism are shown in Chart Vb. With $B = 11$ bonding cluster orbitals ($2a_1 + b_2 + e_3 + e_2 + 2e_1$), $A = 13$ antibonding cluster orbitals ($b_1 + 2e_2 + a_2 + 2e_3 + e_1 + b_2$), and $E = 16$ edges, $X = E - A = 16 - 13 = 3$ can readily be deduced. The energy levels for the pentagonal antiprism are depicted in Chart Vc. With $B = 13$ bonding cluster orbitals ($2a_{1g} + a_{2u} + 2e_{1u} + e_{2g} + e_{1g} + e_{2u}$), $A = 17$ antibonding cluster orbitals ($2e_{2u} + 2e_{2g} + e_{1u} + 2e_{1g} + a_{2g} + a_{1u} + a_{2u}$), and $E = 20$ edges, $X = 20 - 17 = 3$ can be calculated. The additional X value ($X = 1$) for the tetragonal (square) antiprism will be discussed later (under Multiple X Values).

Rule 6. Rule 6 follows directly from the modified Euler theorem, $E = V + F - 2 - S$, where S is the number of shared vertices or edges,[1a] for vertex- and edge-sharing polyhedra. We shall consider one example in each category here. The vertex-sharing bitetrahedral metal cluster (cf. Chart VIa) has been calculated by Ciani and Sironi[14] to have 51 CVMOs. Since CVMO $= 8V_m - F + 2 + X = 8 \times 7 - 8 + 2 + X$, we obtain $X = 1$ as predicted by using the modified Euler theorem ($V = 7$, $F = 8$, $S = 1$). The edge-sharing bitetrahedral metal cluster (cf. Chart VIb) has been calculated by Ciani and Sironi[14] as well as Lauher[8a] to have 43 CVMOs. Since CVMO $= 8 \times 6 - 8 + 2 + X = 43$, we find $X = 1$, in agreement with the prediction from the modified Euler theorem ($V = 6$, $F = 8$, $S = 1$).

Rule 7. For clusters of high nuclearity, small structural perturbations, which amount to relatively small energy changes, can transform the cluster from one polyhedron to another. An example is the transformation of icosahedron to cubocahedron or twinned cuboctahedron. As shown schematically in Chart VII, the cuboctahedron can be visualized as being formed by adding Y electron pairs to an icosahedron, resulting in a lengthening of six metal–metal distances. Since 12 triangular faces are converted to six square faces ($F_2 - F_1 = -6$), the X value for a cuboctahedron becomes $X_2 = X_1 - 6 + Y$ (where X_1 is the X value for the icosahedron). Since each edge of an icosahedron probably corresponds to a metal–metal bond order of less than unity, we expect Y to be $0 \leq Y \leq 6$. The energy level diagrams for the icosahedron and cuboctahedron are shown in Chart VII.[11] With $A = 23$ antibonding and $B = 13$ bonding cluster orbitals and $E = 30$ edges, the icosahedron has an X value of $30 - 23 = 7$. With $A = 23$, $B = 13$, and $E = 24$, the cuboctahedron has an X value of $24 - 23 = 1$. Substituting these X values into the equality $X_2 = 1 = X_1 - 6 + Y = 7 - 6 + Y = 1 + Y$, we obtain $Y = 0$, indicating that the icosahedron and cuboctahedron have similar electron counts, as is indeed observed.[1] The same $X = 1$ value applies to the twinned cuboctahedron, which is related to the cuboctahedron by rotating one of the two triangles about the trigonal symmetry axis by 60°.

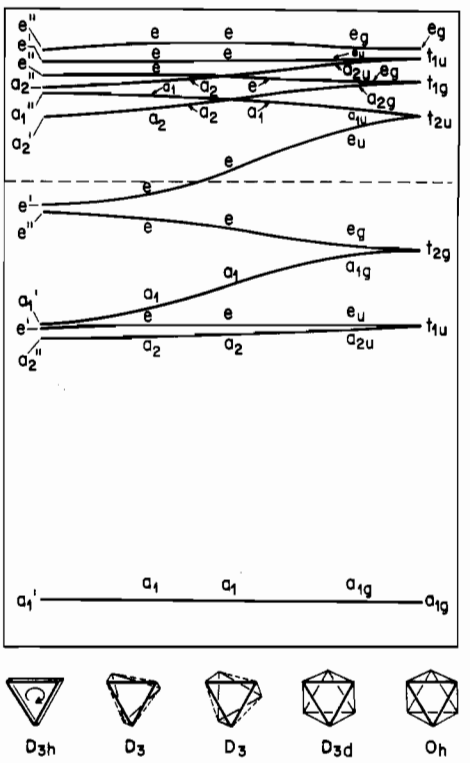

Figure 2. Qualitative correlation (Walsh) diagram (cluster orbitals only) for the conversion of a trigonal prism of D_{3h} symmetry (left) to a trigonal antiprism of D_{3d} symmetry (second from the right) to an octahedron of O_h symmetry (right). Symmetry correlations are given in the text. The four figures on the left depict the successive rotations of one (bottom) of the two triangles of the trigonal prism by 60° to form the trigonal antiprism. A slight shortening of the intertriangle spacing gives rise to the octahedron with 12 equal distances. Note that the word distance refers to interatomic separations whereas the word spacing refers to the interlayer separation (viz., perpendicular distance between the two triangles).

SEP Rules and MO Calculations

The molecular orbital energy level diagram presented in Charts I–VII also provides a theoretical rationale for the skeletal electron pair (SEP) rules; viz., the number of the *skeletal electron pairs* can be given by the number of *bonding cluster orbitals* (B). For example, the closo polyhedra shown in Chart IV and Chart VIIa follow the $B = V + 1$ rule, the nido polyhedra shown in Chart IIIb,c follow the $B = V + 2$ rule, and the arachno polyhedra shown in Chart Vb,c follow the $B = V + 3$ rule. The 3-connected polyhedra shown in Chart I follow the relation $B = E = 3V/2$.[15]

It is also interesting to compare Chart IIa–c with Chart Ia–c. It is readily apparent that the two capping atoms add a total of six (three each) orbitals to the *antibonding* cluster orbital manifold and none to the *bonding* manifold. As a consequence, the number of bonding cluster orbitals (B) remains unchanged as predicted by the *capping* principle.[19]

(14) Ciani, G.; Sironi, A. *J. Organomet. Chem.* **1980**, *197*, 233.

(15) The SEP theory has recently been extended to include 3-connected[16,17] and fused[18] polyhedra.

(16) Evans, D. G.; Mingos, D. M. P. *Organometallics* **1983**, *2*, 435.

(17) Zhang, Q.; Lin, L.; Wang, N.; Lai, S. *Acta Sci. Nat. Univ. Amoi* **1981**, *20*, 226.

(18) (a) Mingos, D. M. P. *J. Chem. Soc., Chem. Commun.* **1983**, 706. (b) Mingos, D. M. P. *J. Organomet. Chem.* **1983**, *251*, C13.

Correlation and Interaction Diagrams

We shall now consider the correlation (Walsh) and interaction diagrams for various polyhedral transformations. We shall focus our attention on the cluster orbital framework only.

Prisms to Antiprisms. Figure 2 depicts a qualitative correlation diagram for the transformation of a trigonal prism of D_{3h} symmetry (left) to a trigonal antiprism of D_{3d} symmetry (second from the right), or an octahedron of O_h symmetry (right) if all 12 edges are equal (right), via rotation of one (bottom) of the triangles by 60°. Note that intermediate (twisted) geometries conform to D_3 symmetry (see the caption for Figure 2 for details of geometrical transformation). The correlations from D_{3h} (trigonal prism) to D_3 (twisted) are as follows: a_1' or $a_1'' \rightarrow a_1$; a_2' or $a_2'' \rightarrow a_2$; e' or e'' → e. It seen that, by twisting the trigonal prism (from left to right in Figure 2), the doubly degenerate, highest occupied cluster orbitals, e', under D_{3h} symmetry become destabilized in energy. This is so because e' is antibonding within the triangles (viz., intralayer antibonding) and bonding between the triangles (viz., interlayer bonding). In the process of the specified deformation, the intralayer interactions remain more or less unaffected but the interlayer interaction is significantly weakened (note also that intralayer distances remain the same while interlayer distances lengthen substantially). In fact, all orbitals that are interlayer bonding (antibonding) will be destabilized (stabilized) due to the increasing loss of interlayer interactions as a result of twisting (cf. Figure 2, from left to right). Another important feature to note is that the HOCO, e', starts out as a bonding orbital under D_{3h} symmetry (since interlayer bonding outweighs intralayer antibonding), destabilizes in energy, and at some halfway point crosses the energy zero (dashed line) to become an antibonding e orbital (the LUCO for a twisted trigonal antiprism or a twisted octahedron). Eventually the e orbitals merge with another antibonding a_1 orbital (originating from a_1'' under D_{3h} symmetry) to form t_{2u} in the octahedron of O_h symmetry. Other orbitals can be understood in a similar manner.

Going in the opposite direction (from right to left, Figure 2), a slight increase in the intertriangle spacing of an octahedron to that in the trigonal prism will lower the symmetry from O_h to the D_{3d} of a trigonal antiprism. A twisting of the trigonal antiprism further lowers the symmetry to D_3. The symmetry correlations for $O_h \rightarrow D_{3d} \rightarrow D_3$ are $a_{1g} \rightarrow a_{1g} \rightarrow a_1$, $e_g \rightarrow e_g \rightarrow e$, $t_{1g} \rightarrow a_{2g} + e_g \rightarrow a_2 + e$, $t_{1u} \rightarrow a_{2u} + e_u \rightarrow a_2 + e$, $t_{2g} \rightarrow a_{1g} + e_g \rightarrow a_1 + e$, $t_{2u} \rightarrow a_{1u} + e_u \rightarrow a_1 + e$, etc., as shown in Figure 2 (from right to left). For example, the LUCO, t_{2u}, under O_h symmetry split into a_{1u} and e_u under D_{3d} symmetry, which correlate with a_1 and e under D_3 symmetry, respectively. If the doubly degenerate (e_u or e) orbitals lie lower in energy than the nondegenerate (a_{1u} or a_1) orbital, they become the lowest unoccupied cluster orbitals for a regular or a twisted trigonal antiprism. Depending upon the interlayer spacing (trigonal antiprism) or the degree of structural deformation (twisted trigonal antiprism), the e orbitals may become weakly antibonding or nearly nonbonding (with energies close to the energy zero). In fact, the e orbitals may play an important role in determining the electron counts of the trigonal prism and antiprism (cf. Multiple X Values).

The net result of the structural transformation of a trigonal prism (D_{3h}) to a trigonal antiprism (D_{3d}) or an octahedron (O_h) via twisting (D_3) is to transfer two orbitals from the bonding (e' under D_{3h}, e under D_3) to the antibonding (e under D_3, e_u under D_{3d}, t_{2u} under O_h) manifold. The number of *bonding* cluster orbitals therefore decreases from 9 to 7, and the corresponding number of *antibonding* cluster orbitals increases from 9 to 11 as shown schematically in Chart VIIIa. Both the trigonal prism and the trigonal antiprism (or the octahedron) have $V = 6$ vertices and hence $3V = 18$ cluster orbitals. For the 3-connected trigonal prism, the 18 cluster orbitals partition into $B = 9$ bonding and $A = 9$ antibonding orbitals. Consequently, it has $B = 9$ skeletal electron pairs, corresponding to the $E = 9$ edges, and $X = E - A = 9 - 9 = 0$. Hence the EAN rule works. For the trigonal antiprism (or octahedron), on the other hand, the 18 cluster orbitals partition into $B = 7$ bonding and $A = 11$ antibonding orbitals. The number of bonding cluster orbitals ($B = 7$) no longer corresponds to the number of edges ($E = 12$); hence, the EAN rule fails, and an X value of $X = E - A = 12 - 11 = 1$ can be deduced.

Chart VIII

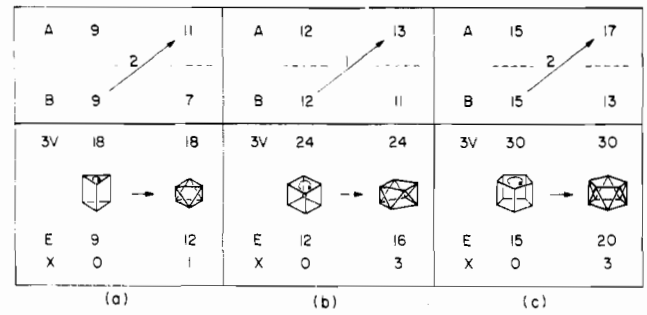

A similar argument applies to the correlation of other prisms and antiprisms. As illustrated in Chart VIIIb, a rotation by 45° of one of the two squares of a square prism (or a cube if all 12 edges are of equal length) gives rise to a square antiprism with 16 edges. In such a process, one orbital is transferred from the *bonding* to the *antibonding* manifold. For the 3-connected square prism, the 24 cluster orbitals partition equally into $B = 12$ and $A = 12$, corresponding to the 12 edges. Hence, the EAN rule works. For the square antiprism, $B = 11$ no longer corresponds to the number of edges ($E = 16$); the EAN rule fails, and $X = E - A = 3$ is obtained.

Also shown in Chart VIIIc is the conversion of a pentagonal prism to a pentagonal antiprism via a rotation of 36° of one of the two pentagons. In the process, two cluster orbitals are transferred from the *bonding* to the *antibonding* regime. For the pentagonal prism, $A = B = E = 15$, $X = E - A = 0$; hence, the EAN rule works. For the pentagonal antiprism, $B = 13$, $A = 17$, and $E = 20$ and hence the EAN rule fails; the discrepancy between E and A is $X = 3$.

It is interesting to note that prisms with a C_n symmetry axis where n = odd (even) transfer an even (odd) number of cluster orbitals from the *bonding* to the *antibonding* manifold in the process of transforming into the corresponding antiprisms.

Pyramids to Bipyramids. The interaction diagram (cluster orbitals only) for capping one of the faces of a tetrahedron (of T_d symmetry) with an atom to form a trigonal bipyramid (of D_{3h} symmetry) is shown in Figure 3. The twelve cluster orbitals of a tetrahedron symmetrize to give six bonding ($a_1 + t_2 + e$) and six antibonding ($t_1 + t_2$) orbitals with an energy ordering shown on the left. As the capping atom approaches the tetrahedron, the symmetry is lowered to C_{3v}, under which the t_1 and t_2 orbitals split into $a_2 + e$ and $a_1 + e$, respectively. The major interaction of the tetrahedron with the capping atom, which has three atomic orbitals of $a_1 + e$ symmetry representations, is via the totally symmetric, bonding a_1 cluster orbital and the weakly bonding, doubly degenerate e cluster orbital, forming three bonding and three antibonding orbitals. Formally, one can view the three resulting bonding cluster orbitals ($a_1 + e$) as tetrahedron based and their antibonding ($a_1 + e$) counterparts as capping-atom based since the tetrahedron contributes three cluster orbitals that are already bonding and hence lie lower in energy and the capping atom contributes three atomic orbitals that lie near the energy zero. In other words, the three bonding orbitals contributed by the tetrahedron are further stabilized and the three atomic orbitals of the capping atom are destabilized and become antibonding in nature as a result of the capping interaction. The net outcome is that the total number ($B = 6$) of bonding cluster orbitals ($a_1 + a_1 + e + e$) in the trigonal bipyramid remains the same as that in the tetrahedron while the total number ($A = 9$) of the antibonding cluster orbitals increases by 3 (with the added $a_1 + e$ orbitals from the capping atom). This is shown schematically in

(19) (a) Mingos, D. M. P. *Nature (London), Phys. Sci.* **1972**, *236*, 99. (b) Forsyth, M. I.; Mingos, D. M. P. *J. Chem. Soc., Dalton Trans.* **1977**, 610.

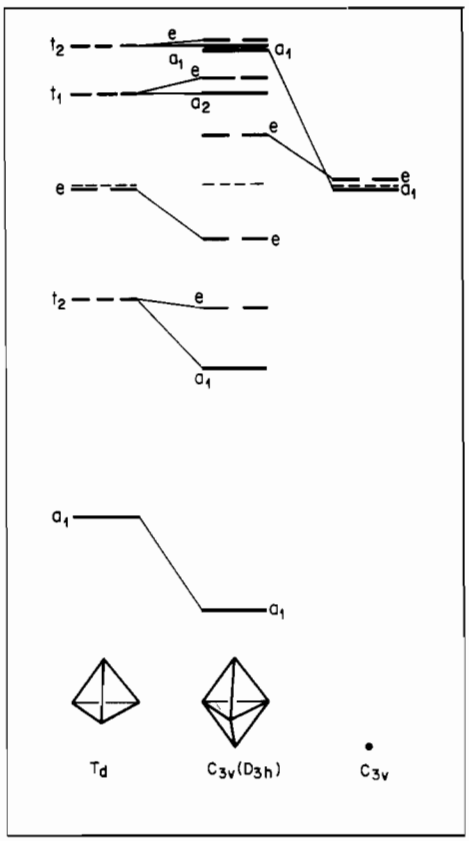

Figure 3. Interaction diagram (cluster orbitals only) for monocapping a tetrahedron (or a trigonal pyramid) with an atom to form a trigonal bipyramid. Symmetry correlations are given in the text. For convenience, orbital symmetry representations under the C_{3v} point group are given for the capping interaction. Splittings of the cluster orbitals of the tetrahedron of T_d symmetry are also indicated.

Chart IX

A	6	+3 → 9	A	8	+3 → 11	A	10	+3 → 13
B	6	6	B	7	7	B	8	8
3V	12	15	3V	15	18	3V	18	21
E	6	9	E	8	12	E	10	15
X	0	0	X	0	1	X	0	2
	(a)			(b)			(c)	

Chart IXa (cf. Charts IIIa and IVa).

The same principle can easily be applied to the transformation of a square pyramid to an octahedron (Chart IXb; cf. Charts IIIb and IVb) or a pentagonal pyramid to a pentagonal bipyramid (Chart IXc; cf. Charts IIIc and IVc). It can be concluded that, for the pyramid to bipyramid transformation (or more generally for monocapping of any given polyhedron), the number of bonding cluster orbitals (B) remains the same[19] while the number of antibonding orbitals (A) increases by 3.

Prisms to Bicapped Prisms. The fact that monocapping a polyhedron gives rise to no change in the number of *bonding* cluster orbitals (B) but an increase of 3 in the number of *antibonding* cluster orbitals has been discussed in the previous subsection. Bicapping of the prisms is illustrated in Chart X. It is easily seen the same principle holds except that A now increases by $2 \times 3 = 6$ for the two caps.

Physical Significance of X, A, and B

We have thus far interpreted parameter X as the number of "missing" antibonding cluster orbitals or, more accurately, as the difference ($E - A$) between the number of edges (E) and the

Chart X

A	9	+6 → 15	A	12	+6 → 18	A	15	+6 → 21
B	9	9	B	12	12	B	15	15
3V	18	24	3V	24	30	3V	30	36
E	9	15	E	12	20	E	15	25
X	0	0	X	0	2	X	0	4
	(a)			(b)			(c)	

number of antibonding cluster orbitals derivable from MO calculations. For systems with multiple X values (as we shall see in the next section), this meaning ($X = E - A$) is lost. However, if one redefines A and B as the number of the *unoccupied* (A') and the *occupied* (B') cluster orbitals, then $X' = E - A'$ and eq 9–12 remain valid with X', A', and B' in place of X, A, and B, respectively. Unless stated otherwise, we shall use the former definition of X, A, and B throughout this paper.

One utility of the TEC rule is that the parameter X can be used to predict the number of antibonding (A) and bonding (B) cluster orbitals (or the number of unoccupied (A') and filled (B') orbitals for systems with multiple X values) in the absence of molecular orbital calculations. Conversely, where such calculations are available, comparisons can be made as to the accuracy of the rules. In Table II the A and B values for a variety of polyhedra are calculated from the parameter X. These calculated values compare favorably well with molecular orbital calculations in the literature.[8,11-14] The comparison of predicted and observed electron counts has already been discussed in our previous papers.[1,2]

It should also be pointed out that antibonding cluster orbitals are often more easily identifiable than their bonding counterparts (where extensive symmetry mixing with other "exo" orbitals may occur) in MO calculations, especially for complicated metal cluster systems.[20] This is one of the reasons we choose to focus our attention on the antibonding manifold.

A distinction should be made here between *cluster* orbitals and *molecular* orbitals. Cluster orbitals are, by definition, molecular orbitals that are responsible for cluster bonding. Hence, the highest occupied molecular orbitals (HOMO) or the lowest unoccupied molecular orbitals (LUMO) of a cluster may or may not be a cluster orbital as we shall see in the next section.

Multiple X Values

The TEC theory allows for multiple electron counts for certain types of polyhedral clusters. This is particularly important since metal clusters often exhibit multiple electron counts either with or without significant structural distortions.

Multiple electron counts can occur for many reasons. On the one hand, electrons may enter or come out of molecular orbitals that are *not* cluster orbitals. Examples of such orbitals are metal–ligand bonds or lone pairs as we shall see below (cf. Octahedron). For these systems, the HOMO or the LUMO is not a cluster orbital. The resulting electron counts will not be directly related to parameters A, B, or X discussed here.

On the other hand, multiple electron counts may arise when some energetically low-lying antibonding *cluster* orbitals are occupied (resulting in higher X values) or when some energetically high-lying bonding cluster orbitals are vacant (resulting in lower X values). In such cases, parameters A and B correspond to the number of vacant and filled cluster orbitals, respectively, and parameter X is still equal to $E - A$. When these orbitals are essentially nonbonding, no significant structural distortion is expected. In contrast, if the occupied cluster orbitals are antibonding (bonding), lengthening (shortening) of appropriate atom pairs is

(20) For discussions on the importance of antibonding cluster orbitals, see, for example: (a) Teo, B. K. Ph.D. Thesis, University of Wisconsin (Madison), 1973. (b) Mingos, D. M. P. *J. Chem. Soc., Dalton Trans.* **1974**, 133.

Table II. Calculations of A and B from X

no.	polyhedron	V	F	X	B	A	no.	polyhedron	V	F	X	B	A
1	tetrahedron	4	4	0	6	6	68	pentacapped trigonal prism	11	18	2	8^a	25^a
				−2	4^a	8^a					3	9	24
2	trigonal bipyramid (hexadeltahedron)	5	6	0	6	9					4	10	23
				2	8^a	7^a	69	tricapped ($\square^3$) cube with two face diagonals	11	17	3	10	23
3	square pyramid	5	5	0	7	8	70	capped ($\square$) square-face-sharing trigonal prism and square antiprism	11	16	2	10^a	23^a
4	hinged butterfly	5	4	0	8	7					3	11	22
5	bicapped tetrahedron or capped trigonal bipyramid	6	8	0	6	12					4	12^a	21^a
				2	8^a	10^a	71	octadecahedron	11	18	5	11	22
6	octahedron	6	8	0	6^a	12^a	72	convex octadecahedron	11	18	6	12	21
				1	7	11	73	tricapped cube	11	15	3	12	21
				3	9^a	9^a	74	capped pentagonal antiprism	11	16	5	13	20
7	trigonal antiprism	6	8	1	7	11	75	capped pentagonal prism	11	11	2	15	18
8	capped square pyramid	6	7	0	7	11	76	hexacapped octahedron	12	20	1	7	29
9	edge-shared bitetrahedron	6	8	1	7	11	77	bidiminished ν_2 trigonal bipyramid (hcp)	12	20	2	8	28
10	octahedron with one edge missing (nido pentagonal bipyramid)	6	7	1	8	10					5	11^a	25^a
11	pentagonal pyramid	6	6	0	8	10	78	face-sharing trioctahedron	12	20	3	9	27
12	trigonal prism	6	5	0	9	9	79	face-sharing bi(square antiprism)	12	18	2	10^a	26^a
				−2	7^a	11^a					6	14	22
13	tricapped tetrahedron or bicapped trigonal bipyramid	7	10	0	6	15	80	capped ($\square$) fused trigonal prism–square antiprism–trigonal bipyramid	12	18	1	9^a	27^a
				2	8	13					3	11	25
14	bicapped square pyramid	7	9	0	7	14					5	13^a	23^a
15	capped octahedron	7	10	1	7	14	81	icosahedron	12	20	7	13	23
16	pentagonal bipyramid (decadeltahedron)	7	10	2	8	13					3	9^a	27^a
17	capped ($\triangle$) trigonal prism	7	7	0	9	12	82	cuboctahedron (ccp)	12	14	1	13	23
18	capped ($\square$) trigonal prism	7	8	1	9	12	83	twinned cuboctahedron (hcp)	12	14	1	13	23
19	hexagonal pyramid	7	7	0	9	12	84	hexagonal antiprism	12	14	3	15	21
20	$3^1 5^3$ tetrahedron	7	4	0	12	9	85	bicapped pentagonal prism	12	15	4	15	21
21	tetracapped tetrahedron	8	12	0	6	18	86	triangular-face sharing tri(trigonal prism)	12	11	0	15	21
22	bicapped octahedron	8	12	1	7	17	87	face-sharing dicube	12	10	0	16	20
23	fused octahedron and trigonal bipyramid	8	12	1	7	17	88	hexagonal prism	12	8	0	18	18
				3	9^a	15^a	89	3-connected ν_3 truncated tetrahedron ($3^4 6^4$ octahedron)	12	8	0	18	18
24	triangulated dodecahedron (dodecadeltahedron)	8	12	1	7^a	17^a	90	$4^4 5^4$ octahedron	12	8	0	18	18
				2	8^a	16^a	91	heptacapped octahedron	13	22	1	7	32
				3	9	15	92	monodiminished ν_2 trigonal bipyramid	13	22	2	8	31
25	bicapped ($\triangle^2$) trigonal prism	8	9	0	9	15					5	11^a	28^a
26	bicapped ($\triangle$,$\square$) trigonal prism	8	10	1	9	15	93	capped face-sharing trioctahedron	13	22	3	9	30
27	bicapped ($\square^2$) trigonal prism	8	11	1	8^a	16^a	94	capped ($\square$) face-sharing bi(square antiprism)	13	21	3	10^a	29^a
				2	9	15					7	14	25
				3	10	14	95	pentacapped cube	13	21	5	12	27
28	hexagonal bipyramid	8	12	3	9	15	96	capped ($\triangle$) cuboctahedron	13	16	1	13	26
29	heptagonal pyramid	8	8	0	10	14	97	capped ($\square$) cuboctahedron	13	17	2	13	26
30	square-face-sharing bitrigonal prism	8	8	0	10	14	98	capped ($\triangle$) twinned cuboctahedron	13	16	1	13	26
31	square antiprism	8	10	1	9^a	15^a	99	capped ($\square$) twinned cuboctahedron	13	17	2	13	26
				3	11	13	100	capped ($\bigcirc$) hexagonal antiprism	13	19	6	15	24
32	cube (hexahedron)	8	6	0	12	12	101	capped face-sharing dicube	13	13	1	16	23
33	cuneane	8	6	0	12	12	102	capped ($\bigcirc$) hexagonal prism	13	13	3	18	21
34	tricapped octahedron	9	14	1	7	20	103	octacapped octahedron (face-centered cube)	14	24	1	7	35
35	face-sharing bioctahedron	9	14	2	8	19	104	ν_2 trigonal bipyramid	14	24	2	8	34
36	heptagonal bipyramid	9	14	4	10	17					5	11^a	31^a

37	tricapped ($\triangle^2$,□) trigonal prism	9	12	1	9	18	105	bicapped (□²) face-sharing bi(square antiprism)	14	24	4	10[a]	32[a]
38	tricapped ($\triangle$,□²) trigonal prism	9	13	2	9	18					8	14	28
39	tricapped (□³) trigonal prism (tetracaidecadeltahedron)	9	14	2	8[a]	19[a]	106	hexacapped cube	14	24	6	12	30
				3	9	18	107	bicapped ($\triangle^2$) cuboctahedron	14	18	1	13	29
				4	10	17	108	rhombic dodecahedron (bcc)	14	"24"	>6	>12	<30
40	capped ($\triangle$) square antiprism	9	12	1	9[a]	18[a]	109	bicapped hexagonal antiprism	14	24	9	15	27
				3	11	16	110	tetracapped (□², ⬠²) pentagonal prism	14	21	6	15	27
41	capped (□) square antiprism	9	13	2	9[a]	18[a]	111	bicapped (□²) face-sharing dicube	14	16	2	16	26
				4	11	16	112	heptagonal antiprism	14	16	3	17	25
42	$3^{11}5^1$ dodecahedron (nido bicapped square antiprism)	9	12	1	9[a]	18[a]	113	bicapped (⬡²) hexagonal prism	14	18	6	18	24
				3	11	16	114	heptagonal prism	14	9	0	21	21
43	face-sharing octahedron and trigonal prism	9	11	1	10	17	115	4^35^6 nonahedron	14	9	0	21	21
44	tricapped (□³) trigonal prism with elongated interlayer edges	9	11	2	11[a]	16[a]	116	capped heptagonal antiprism	15	22	7	17	28
				3	12[a]	15[a]	117	triangular face-sharing tetra(trigonal prism)	15	14	0	18	27
				4	13[a]	14[a]	118	capped heptagonal prism	15	15	4	21	24
45	3^85^2 decahedron	9	10	1	11	16	119	corner-sharing dicube	15	12	1	21	24
46	triangular face sharing bi(trigonal prism)	9	8	0	12	15	120	face-sharing tri(square antiprism)	16	26	3	11[a]	37[a]
47	capped cube	9	9	1	12	15					9	17	31
48	capped (□) cuneane	9	9	1	12	15	121	face-sharing tricube	16	14	0	20	28
49	capped (⬠) cuneane	9	10	2	12	15	122	4^66^4 decahedron (truncated bisphenoid)	16	10	0	24	24
50	3^55^3 octahedron	9	8	1	13	14	123	4^25^8 decahedron	16	10	0	24	24
51	ν_2 tetrahedron (tetracapped octahedron)	10	16	1	7	23	124	heptacapped pentagonal prism	17	30	9	15	36
52	tetracapped ($\triangle^2$,□²) trigonal prism	10	15	2	9	21	125	bicapped face-sharing bi(pentagonal antiprism)	17	30	10	16	35
53	tetracapped ($\triangle$,□³) trigonal prism	10	16	2	8[a]	22[a]	126	bicapped pentagonal face-sharing bi(pentagonal prism)	17	20	4	20	31
				3	9[a]	21[a]	127	hexacapped ($\triangle^6$) cuboctahedron	18	26	1	13	41
				4	10	20	128	hexacapped (□⁶) cuboctahedron or ν_2 octahedron	18	32	7	13	41
54	bicapped (□²) square antiprism (heccaidecadeltahedron)	10	16	3	9[a]	21[a]	129	hexacapped ($\triangle^6$) twinned cuboctahedron	18	26	1	13	41
				5	11	19	130	hexacapped (□⁶) twinned cuboctahedron	18	32	7	13	41
55	edge-sharing bioctahedron	10	16	3	9	21	131	$4^25^86^1$ undecahedron	18	11	0	27	27
56	$B_{10}H_{14}$-type (nido octadecahedron)	10	13	2	11[a]	19[a]	132	capped (⬠) $4^25^86^1$ undecahedron	19	16	3	27	30
				3	12	18	133	pentagonal dodecahedron	20	12	0	30	30
57	bicapped cube	10	12	2	12	18							
58	bicapped (⬠²) cuneane (sphenocorona)	10	14	4	12	18							
59	capped ($\triangle$) 3^55^3 octahedron	10	10	1	13	17							
60	capped (⬠) 3^55^3 octahedron	10	12	3	13	17							
61	pentagonal antiprism	10	12	3	13	17							
62	pentagonal prism	10	7	0	15	15							
63	$3^35^36^1$ heptahedron (diademane-type)	10	7	0	15	15							
64	$3^14^35^3$ heptahedron	10	7	0	15	15							
65	pentacapped octahedron	11	18	1	7	26							
66	face-to-face fused trioctahedron	11	18	2	8	25							
67	face-to-face fused trioctahedron without central edge	11	18	3	9	24							

[a] See text (under the heading Multiple X Values). Note that these B and A values correspond to the number of the filled and the vacant cluster orbitals, respectively.

expected and vice versa for vacant cluster orbitals. Accompanying such bond lengthening or shortening may be a systematic distortion of the cluster to a lower symmetry (subgroup) via vibronic (Jahn–Teller) interactions. We shall discuss some of the systems with multiple X values.

Tetrahedron. Since the highest occupied cluster orbital (HOCO) of e symmetry (cf. Chart IIIa) in the tetrahedron is weakly bonding (reason: formed by tangential atomic orbitals), it might be expected that some tetrahedral clusters may be electron deficient with four electrons (i.e. with the doubly degenerate e orbital vacant) less than expected. One example of such a cluster is $Re_4(CO)_{12}H_4$[21] with four face-bridging hydrides. This tetrametal cluster has $4 \times 7 + 12 \times 2 + 4 \times 1 = 56$ electrons, 4 electrons less than the expected value of $N = 2(8V_m - F + 2 + X) = 2(8 \times 4 - 4 + 2 + 0) = 60$ electrons (cf. eq 6). Another example is B_4Cl_4[22] which has $4 \times 3(B) + 4 \times 1$ (Cl) = 16 electrons, 4 less than the expected value of $N = 2(3V_n - F + 2 + X) = 2(3 \times 4 - 4 + 2 + 0) = 20$ electrons. In the latter case, however, there is strong evidence[23] that the B–Cl bonds contain multiple-bond character so as to compensate for the electron deficiency. Nevertheless, the X value for these electron-deficient tetrahedral clusters appears to be, formally, $X = -2$.

Trigonal Bipyramid. The TEC rule predicts two X values for trigonal bipyramids (cf. rule 4). We have already discussed one of them, $X = 0$, in Chart IVa. The higher X value, $X = 2$, predicted by the inverted Hückel diagram, can be obtained by populating the doubly degenerate lowest unoccupied cluster orbitals (LUCO) e′ (cf. Chart IVa), thereby giving rise to an electron-rich cluster with four electrons more than expected. This is indeed observed in, for example, $[Pd_2P_3L_2]^+$ (L = 1,1,1-tris((diphenylphosphino)methyl)ethane)[24] and $[Ni_5(CO)_{12}]^{2-}$.[25] Since the LUCO e′ orbitals in the regular trigonal bipyramid are highly antibonding as suggested by MO calculations (Hoffmann and Lipscomb,[11] Lauher[8a]), a significant distortion is expected for these electron-rich clusters. Indeed, $[Ni_5(CO)_{12}]^{2-}$, for example, exhibits significantly longer axial–equatorial than equatorial–equatorial distances. A correlation diagram for such elongation can be found in Lauher's work (Figure 5 in ref 8a).

Octahedron (Tetragonal Bipyramid). The TEC theory predicts two X values for the tetragonal bipyramid: $X = 1, 3$. In Chart IVb (see also Figure 2), the energy level diagram for the octahedron is shown, corresponding to $X = 1$. Most octahedral clusters conform to $X = 1$ and $B = 7$. Octahedral metal clusters with $X = 3$ (formally) have been observed in, e.g., $Ni_6(\eta^5\text{-}C_5H_5)_6$[26] and $Fe_6S_8(PEt_3)_6^{2+}$.[27] These two clusters do not exhibit significant structural distortion. The absence of such distortion may be due to steric constraints imposed by the ligands, substantial metal–ligand antibonding character in the HOMO, or high spin states. In fact, the latter cluster has been reported to have six unpaired electrons.[27b]

In this paper, we assume that each metal atom, as in the case of main-group elements, contributes three *hybrid* orbitals for cluster bonding. In terms of local site symmetry, they can be classified as one σ_z (pointing inward) and two π_x, π_y (pointing tangentially) orbitals. All other metal orbitals are either engaged in metal–ligand bonding or completely filled to give lone pairs. For example, each metal atom in the octahedral cluster $Rh_6(CO)_{16}$ uses four orbitals for bonding with two terminal and two triply

Chart XI

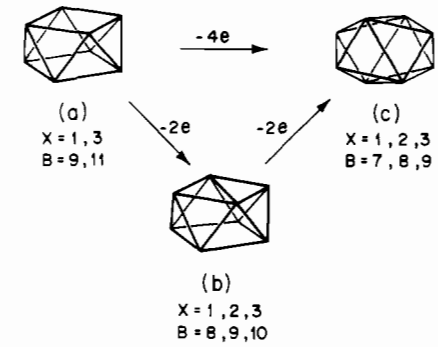

bridging carbonyls. The remaining five orbitals of σ_z, π_x, π_y, $\delta_{x^2-y^2}$, and δ_{xy} local symmetry are available for cluster bonding. The 18 $\sigma_z\,\pi_x\,\pi_y$ orbitals give rise to 7 bonding and 11 antibonding cluster orbitals (cf. Chart IVb). The 12 δ-type orbitals give rise to an energetically closely spaced manifold of weakly bonding or antibonding orbitals. The degree of orbital interaction follows the expected order $\sigma \gg \pi \gg \delta$. For $Rh_6(CO)_{16}$, all 12 δ orbitals are filled, giving rise to 12 lone pairs. The 43 electron pairs can thus be formally partitioned as follows: 12 terminal Rh–C bonds, 12 bridging Rh–C bonds, 7 bonding cluster orbitals, and 12 Rh lone pairs.

As stated earlier, multiple electron counts can arise when the δ-orbital manifold ("lone pairs") is partially, instead of fully, filled as is often found in early-transition-metal clusters such as $[Mo_6Cl_{14}]^{2-}$[28a] and $[Nb_6Cl_{18}]^{n-}$, where $n = 2$[28b] and 4.[28c] Each metal atom in these clusters is bonded to one terminal and four bridging ligands, leaving four orbitals for metal–metal interaction. For $[Mo_6Cl_{14}]^{2-}$, the 42 electron pairs can formally be classified as follows: 6 terminal Mo–Cl bonds, 24 face-bridging Mo–Cl bonds, 7 bonding cluster orbitals, and 5 $\delta_{x^2-y^2}$ orbitals. For $[Nb_6Cl_{18}]^{2-}$, the 37 electron pairs can formally be assigned to the following: 6 terminal Nb–Cl bonds, 24 edge-bridging Nb–Cl bonds, and 7 bonding cluster orbitals. And for $[Nb_6Cl_{18}]^{4-}$, one extra pair of electrons enters the δ_{xy} manifold.

Trigonal Prism. The majority of trigonal-prismatic clusters conform to $X = 0$ and $B = 9$ (cf. Chart Ia). If the highest occupied cluster orbital (HOCO) e′ is vacant, one might expect an electron-deficient system with $X = -2$ and $B = 7$, viz., four electrons less than expected. This is possible because the HOCO e′ orbitals are only weakly bonding, and a twisting or a slipping deformation may cause the e′ orbitals to rise in energy such that they become vacant. This may be observed in the $[Pt_6(CO)_{12}]^{2-}$ dianion,[29a] which has a slipped trigonal-prismatic structure with 86 rather than 90 electrons. The reason for such electron deficiency, however, is more likely related to the tendency of platinum to conform to a 16- rather than to an 18-electronic configuration and the HOMO is probably predominantly carbonyl π^* in nature.[29b]

Square Antiprism. Since the highest occupied cluster orbital in square antiprism (Chart XIa) is the doubly degenerate orbital e_1 (cf. Chart Vb), it might be expected that some electron-deficient square-antiprismatic clusters with four electrons less than that predicted for $X = 3$ may be found. These systems, with the energetically high-lying HOCO e_1 vacant, correspond formally to $X = 1$. Indeed, these are quite common among metal clusters. For example, $[Ni_8C(CO)_{16}]^{2-}$,[30] with 118 electrons, conforms to

(21) (a) Saillant, R.; Barcelo, G.; Kaesz, H. D. *J. Am. Chem. Soc.* **1970**, *92*, 5739. (b) Wilson, R. D.; Bau, R. *Ibid.* **1976**, *98*, 4687. (c) Hoffmann, R.; Schilling, B. E. R.; Bau, R.; Kaesz, H. D.; Mingos, D. M. P. *Ibid.* **1978**, *100*, 6088.
(22) Atoji, M.; Lipscomb, W. N. *Acta Crystallogr.* **1953**, *6*, 547.
(23) See, for example, ref 3 and the following: Wong, E. H.; Kabbani, R. M. *Inorg. Chem.* **1980**, *19*, 451.
(24) Dapporto, P.; Sacconi, L.; Stoppioni, P.; Zanobini, F. *Inorg. Chem.* **1981**, *20*, 3834.
(25) Longoni, G.; Chini, P.; Lower, L. D.; Dahl, L. F. *J. Am. Chem. Soc.* **1975**, *97*, 5034.
(26) Paquette, M. S.; Dahl, L. F. *J. Am. Chem. Soc.* **1980**, *102*, 6621.
(27) (a) Cecconi, F.; Ghilardi, C. A.; Middolini, S. *J. Chem. Soc., Chem. Commun.* **1981**, 640. (b) Agresti, A.; Bacci, M.; Cecconi, F.; Ghilardi, C. A.; Midollini, S. *Inorg. Chem.* **1985**, *24*, 689 and references cited therein for related cobalt clusters.
(28) (a) Schäfer, H.; Schnering, H. G.; Tillack, J.; Kuhnen, F.; Wöhrle, H.; Baumann, H. *Z. Anorg. Allg. Chem.* **1967**, *353*, 281. (b) Field, R. A.; Kepert, D. L.; Robinson, B. W.; White, A. H. *J. Chem. Soc., Dalton Trans.* **1973**, 1858. (c) Simon, A.; Schnering, H. G. *Z. Anorg. Allg. Chem.* **1968**, *361*, 235.
(29) (a) Calabrese, J. C.; Dahl, L. F.; Chini, P.; Longoni, G.; Martinengo, S. *J. Am. Chem. Soc.* **1974**, *96*, 2614. (b) Hoffmann, R., private communication.
(30) (a) Longoni, G.; Ceriotti, A.; Della Pergola, R.; Manassero, M.; Perego, M.; Piro, G.; Sansoni, M. *Philos. Trans. R. Soc. London, Ser. A* **1982**, *A308*, 47. (b) Ceriotti, A.; Longoni, G.; Manassero, M.; Perego, M.; Sansoni, M. *Inorg. Chem.* **1985**, *24*, 117.

$X = 3$ whereas the electron-deficient $[Co_8C(CO)_{18}]^{2-}$,[31] with 114 electrons, corresponds to $X = 1$. The latter cluster shows a rhombic distortion of the two square faces. Hence, the TEC theory[1,2] predicts two X values ($X = 1, 3$) for the square antiprism via the Hückel molecular orbital energy diagram (cf. Table I).

Bicapped (C_{2v}) Trigonal Prism. The trigonal prism with two square caps (cf. Chart XIb) is predicted to have three possible X values; $X = 2$ via rule 2 (capping two square faces of a trigonal prism) and $X = 1, 3$ via rule 7 (removal of two electrons from one square face of a square antiprism to give two trigonal faces). $X = 3$ was observed in B_8H_{12},[3] corresponding to $B = 10$. Note that the concept of characterizing a cluster as electron rich, electron precise, and electron deficient begins to break down even for the octavertex cluster discussed here as well as in the next subsection. Both $X = 2$ and $X = 3$ can be considered as electron precise since the former is derived from the electron-precise trigonal prism while the latter is based on the electron-precise square antiprism. The case of $X = 1$ is electron deficient on both counts.

Triangular Dodecahedron. The TEC theory predicts multiple X values for the triangular dodecahedron (Chart XIc): $X = 1$, 3 from the square antiprism via removal of four electrons (thereby converting two square faces to four triangular faces) or $X = 1$, 2, 3 from the bicapped (C_{2v}) trigonal prism via removal of two electrons (thereby transforming the square face into two triangular faces). The observed X values are $X = 2$ as in $Cp_4Co_4B_4H_4$ ($B = 8$),[32] $X = 3$ as in $B_8H_8^{2-}$[3] and $Fe_4(CO)_{11}(HCCEt)_2$[33] ($B = 9$), and $X = 4$ as in $Cp_4Ni_4B_4H_4$[34] ($B = 10$). As in the case of the bicapped (C_{2v}) trigonal prism, both $X = 2$ and $X = 3$ are "electron precise". In this regard, it is interesting to note that Lauher's calculation shows that there are $A = 16$ antibonding cluster orbitals, which corresponds to $B = 8$ and $X = E - A = 18 - 16 = 2$. In contrast, SEP theory predicts $B = V + 1 = 9$, which corresponds to $X = 3$ (cf. Chart XIc).

The bonding for the (metalla) borane clusters described here has also been discussed by King,[35] who showed that the replacement of light atoms (boron and carbon) in eight-vertex deltahedral systems by transition metals leads eventually to a point where deltahedral bonding involving both surface and core interactions is replaced by surface-localized bonding. King's bonding description points to the inadequacy of the two-center two-electron description for these systems.

It is also important to note that $B_8H_8^{2-}$ exists in the solid state[36] as a D_{2d} triangular dodecahedron (Chart XIc). In solution,[37] it is fluxional and NMR shows the coexistence of square-antiprism (D_{4d}) (Chart XIa) and bicapped-trigonal-prism (C_{2v}) (Chart XIb) structures, interconverting via, presumably, the triangular-dodecahedral intermediate.[38] Despite the differences in the number of electrons, we note that all three structures have multiple X values and hence multiple electron counts. The common B value is 9. With the reasonable assumption that the energetics of all three forms are not very different, it is not surprising that all three structures can coexist for the same electron count.

Icosahedron. As shown in Chart VIIa, the HOCO in an icosahedron is the quadruply degenerate g_u orbital. It might be expected that some electron-deficient icosahedral cluster may exist with eight electrons less than expected (with nine orbitals, $a_g + t_{1u} + h_g$, filled and four orbitals, g_u, vacant). The $[Au_{13}Cl_2(PMe_2Ph)_{10}]^{3+}$ trication[39] is such an example. It has 162 electrons,[40] corresponding to $X = 3$ and $B = 9$[40] instead of the expected 170 electrons, which correspond to $X = 7$ and $B = 13$ as exemplified by $[Rh_{12}Sb(CO)_{27}]^{3-}$.[41] In fact, the "spherical" gold clusters[42] such as $[Au_{13}L_{12}]^{5+}$, $[Au_{11}L_{10}]^{3+}$, $[Au_9L_8]^+$, and $[Au_8L_8]^{2+}$ (where L represents phosphine ligands) appear to have $B = 9$[43] while the "toroidal" gold cluster[42] such as $[Au_9L_8]^{3+}$ and $[Au_8L_7]^{2+}$ seem to have $B = 8$.[44] Note that most of these structures are based on, or derivable from, the icosahedral geometry. In either case, the center gold atom is considered as "encapsulated" while the peripheral gold atoms are considered as vertex (V) atoms. Thus, the electron counts for the "spherical" and the "toroidal" gold clusters are $N = 2 \times (6V + 9) = 12V + 18$ and $N = 2 \times (6V + 8) = 12V + 16$, respectively (cf. eq 7). The two are interconvertible via addition or subtraction of two electrons, e.g.[42]

$$Au_9L_8^{3+} \underset{-2e^-}{\overset{2e^-}{\rightleftharpoons}} [Au_9L_8]^+ \qquad [Au_8L_7]^{2+} \underset{-L}{\overset{L}{\rightleftharpoons}} [Au_8L_8]^{2+}$$

Once again, the electron deficiency in these gold clusters is probably related to the tendency of gold to conform to 16- rather than 18-electronic configuration.

Conclusion

It is shown in this paper that the rules for determining the parameter X of the topological electron-counting (TEC) theory can be justified within the framework of molecular orbital theory. In this respect, the parameter X is no longer an "adjustment" factor as was originally developed to make the effective atomic number (EAN) rule work for polyhedral clusters.[1,2] The parameter X can now be interpreted as the number of "missing" *antibonding* cluster orbitals (or more precisely, $X = E - A$) and hence can be derived from molecular orbital calculations.

It is also shown that, within the framework of MO theory, the number of *bonding* cluster orbitals corresponds to the number of skeletal electron pairs in the context of the widely used skeletal electron pair (SEP) theory. Consequently, the TEC rule provides an alternative and complementary way of estimating the number of skeletal electron pairs.

It is obvious that the EAN rule works only when the number of antibonding cluster orbitals (A) is equal to the number of edges (E). The discrepancy is, of course, the parameter $X = E - A$. Electron-counting rules such as SEP and TEC are useful when the parameter X deviates from zero.

It is concluded that both the TEC and the SEP rules can be derived from molecular orbital calculations, many of which can be found in the literature, particularly the pioneering work of Hoffmann and Lipscomb.[11]

Qualitative correlation (Walsh) and interaction diagrams (cluster orbitals only) are constructed for the conversion of prisms to antiprisms, pyramids to bipyramids, and prisms to bicapped prisms.

Multiple X values, and hence multiple electron counts, for certain polyhedral clusters are justified within the framework of

(31) Albano, V. G.; Chini, P.; Ciani, G.; Martinengo, S.; Sansoni, M. *J. Chem. Soc., Dalton Trans.* **1978**, 463.
(32) Pipal, J. R.; Grimes, R. N. *Inorg. Chem.* **1979**, *18*, 257.
(33) Sappa, E.; Tiripicchio, A.; Camellini, M. T. *J. Chem. Soc., Dalton Trans.* **1978**, 419.
(34) Bowser, J. R.; Bonny, A.; Pipal, J. R.; Grimes, R. N. *J. Am. Chem. Soc.* **1979**, *101*, 6229.
(35) King, R. B. *Polyhedron* **1982**, *1*, 133.
(36) (a) Klanberg, F.; Eaton, D. R.; Guggenberger, L. J.; Muetterties, E. L. *Inorg. Chem.* **1967**, *6*, 1271. (b) Guggenberger, L. J. *Inorg. Chem.* **1969**, *8*, 2771.
(37) Muetterties, E. L.; Wiersema, R. J.; Hawthorne, M. F. *J. Am. Chem. Soc.* **1973**, *95*, 7520.
(38) Muetterties, E. L.; Beier, B. F. *Bull. Soc. Chim. Belg.* **1975**, *84*, 397.
(39) Briant, C. E.; Theobald, B. R. C.; White, J. W.; Bell, L. K.; Mingos, D. M. P.; Welch, A. J. *J. Chem. Soc., Chem. Commun.* **1981**, 201.
(40) For $[Au_{13}Cl_2(PMe_2Ph)_{10}]^{3+}$, observed $N = 13 \times 11 + 2 \times 1 + 10 \times 2 - 3 = 162$, $T = N/2 = 81$, and $B = T - 6V = 81 - 6 \times 12 = 9$ (cf. eq 7). Note that V_n or V_m in eq 7 counts only the vertex or peripheral atoms.
(41) Vidal, J. L.; Troup, J. M. *J. Organomet. Chem.* **1981**, *213*, 351.
(42) For reviews of gold phosphine clusters, see, for example: (a) Mingos, D. M. P. *Philos. Trans. R. Soc. London, Ser. A* **1982**, *A308*, 75. (b) Steggerda, J. J.; Bour, J. J.; van der Velden, J. W. A. *Recl. Trav. Chim. Pays-Bas* **1982**, *101*, 164. (c) Briant, C. E.; Hall, K. P.; Wheeler, A. C; Mingos, D. M. P. *J. Chem. Soc., Chem. Commun.* **1984**, 248. (d) van der Velden, J. W. A.; Stadnik, Z. M. *Inorg. Chem.* **1984**, *23*, 2640.
(43) From the procedure outlined in footnote 40, the $[Au_{11}L_{10}]^{3+}$ or the $Au_{11}L_7X_3$ (L = phosphine and X = halogen) clusters have $N = 138$, $T = 69$, and $B = 69 - 6 \times 10 = 9$, the $[Au_9L_8]^+$ clusters have $N = 114$, $T = 57$, and $B = 57 - 6 \times 8 = 9$, and the $[Au_8L_8]^{2+}$ clusters have $N = 102$, $T = 51$, and $B = 51 - 6 \times 7 = 9$.
(44) From the procedure of footnote 40, the $[Au_9L_8]^{3+}$ clusters have $N = 112$, $T = 56$, and $B = 56 - 6 \times 8 = 8$; the $[Au_8L_7]^{2+}$ clusters have $N = 100$, $T = 50$, and $B = 50 - 6 \times 7 = 8$.

MO theory and illustrated with some representative examples.

The distinction between *cluster* orbitals and *molecular* orbitals is emphasized. In particular, the highest occupied or the lowest unoccupied molecular orbitals of a cluster may or may not be cluster orbitals. As a result, there are various causes of multiple electron counts, some involving cluster orbitals, others not. For the latter case, simple electron-counting rules are incapable of discerning the nature and/or predicting the consequences of the added or the subtracted electrons.

Finally, while we have restricted our discussions to clusters containing up to 20 vertex atoms, the principles outlined in this paper can easily be extended to higher clusters.[45]

Acknowledgment. I am indebted to Prof. J. Lauher of SUNY, Stony Brook, for suggesting the alternative interpretation of the parameter X as the number of "false" metal-metal bonds in ref 1a, which provided a seed for the present paper. I am also grateful to Kelly Keating for many helpful comments.

(45) For complications introduced by too much symmetry in electron counting of high-nuclearity clusters, see, for example: (a) Bicerano, J.; Marynick, D. S.; Lipscomb, W. N. *Inorg. Chem.* **1978**, *17*, 3443. (b) Brown, L. D.; Lipscomb, W. N. *Ibid.* **1977**, *16*, 2989.

Contribution from the Department of Chemistry, Kinki University, Kowakae, Higashi-Osaka 577, Japan

Classification of Solvents Based on Their Coordination Power to Nickel(II) Ion. A New Measure for Solvent Donor Ability

MEGUMU MUNAKATA,* SUSUMU KITAGAWA, and MASAHARU MIYAZIMA

Received June 5, 1984

Coordination power (CP), a new measure for the donor ability of a solvent, was determined by using nickel(II) ion and applying the rule of average environment. The values of CP on the basis of acetonitrile are 2.24 (pyridine), 1.24 (dimethyl sulfoxide), 0.85 (*N*,*N*-diethylformamide), 0.79 (water), 0.72 (*N*,*N*-dimethylformamide), 0.11 (methanol), 0.08 (trimethyl phosphate), 0.00 (acetonitrile), −0.07 (*n*-hexanol and *n*-pentanol), −0.12 (ethanol and *n*-butanol), −0.14 (*n*-propanol), −0.15 (propionitrile), −0.37 (benzonitrile), −0.46 (acrylonitrile and isobutyl alcohol), −0.48 (acetone), −0.54 (isopropyl alcohol), −0.68 (*sec*-butyl alcohol), −0.77 (propylene carbonate), and −0.92 (*tert*-butyl alcohol). The stability constants of Mg(II) and Ag(I) complexes with bpy and the Ni(II) complex with 2,9-Me_2phen decrease with the increase of CP. The activation enthalpy for the ligand substitution reaction of nickel(II) ion with bpy increases linearly with the increase of CP in the solvents with the same functional group. The half-wave potentials of the Ni^{2+}/Ni^0 couple in nitrile solvents become more negative with the increase of CP and a good relationship between CP and the ligand field splitting parameter ($10Dq$) for the nickel(II) solvate ion was found. Thus, CP is concluded to be a good measure for the donor ability of the solvents.

Introduction

Chemical reactions in solutions cannot be essentially understood without clarification of the effect of a solvent. An important and urgent problem in the study on the inorganic reaction in solutions is to obtain a measure representing the strength of the interaction between solvent and metal ion. The effects of solvents on the complexation reactions, electrode reactions, catalytic reactions, and syntheses in which metal ions participate should be divided into the solvation effect and the dilution effect to be discussed. The former especially plays an important role in these reactions. Many attempts have been made to correlate observed changes in the reactivity of metal ions with fundamental bulk properties of the solvents involved, such as their dielectric constants, dipole moments, and polarizabilities. Such attempts have met with only limited success.

Gutmann has proposed the donor number, which is the enthalpy change on the solvation of pentachloroantimony(V), as a measure for the basicity of solvents.[1,2] The donor number has served as a useful guide for the interpretation of the solvent effects on the chemical shift of CF_3I,[3] the stability constants of $SbCl_6^{-2}$ and complexes of univalent cations with solvents,[4] the half-wave potentials of metal ions,[5] Mössbauer isomer shifts,[6] and the electron binding energies of the $3d_{5/2}$ orbitals of antimony.[7] But no donor numbers of alcohols, which are frequently used as solvents and are indispensable in the study of nonaqueous chemistry, were reported by Gutmann. The prediction of the donor number of methanol from the solvent dependence of the dissociation rate and the equilibrium constant of the nickel complex with the thiocyanate,[8] the activation for dissociation of the nickel(II) complexes with isoquinoline,[9] and NMR measurement[10] has been attempted. A modified value for it was suggested from a relationship between ESR parameters of bis(2,6-dimethyl-3,5-heptanedionato)copper(II) and the donor numbers of solvents.[11] From kinetic studies on the ligand substitution[12] and the solvent-exchange enthalpies[13a] of nickel(II) ions, it was suggested that the donor numbers did not necessarily apply to such acceptors as nickel(II) ions having covalent bonds.

There is no good measure for the strength of a metal ion–solvent interaction except for the donor number, though we strongly expect to establish a new concept for the classification of a solvent based

(1) Gutmann, V.; Wychera, E. *Inorg. Nucl. Chem. Lett.* **1966**, *2*, 257.
(2) Gutmann, V. "Coordination Chemistry in Non-Aqueous Solution"; Springer-Verlag: New York, 1968.
(3) Spaziante, P.; Gutmann, V. *Inorg. Chim. Acta* **1971**, *5*, 273.
(4) Izutsu, K.; Nakamura, T.; Iwata, K. *Anal. Chim. Acta* **1980**, *117*, 329.
(5) (a) Gutmann, V. *Monatsh. Chem.* **1969**, *100*, 2113. (b) Gutmann, V. *Fortschr. Chem. Forsch.* **1972**, *27*, 59.
(6) Vertes, A.; Burger, K. *J. Inorg. Nucl. Chem.* **1972**, *34*, 3665.
(7) Burger, K.; Fluck, E. *Inorg. Nucl. Chem. Lett.* **1974**, *10*, 171.
(8) Dickert, F.; Hoffmann, H.; Janjic, T. *Ber. Bunsenges. Phys. Chem.* **1974**, *78*, 712.
(9) Chattopandhyay, P. K.; Kratochvil, B. *Inorg. Chem.* **1976**, *15*, 3104.
(10) (a) Erlich, R. H.; Roach, E.; Popov, A. I. *J. Am. Chem. Soc.* **1970**, *92*, 4989. (b) Erlich, R. H.; Popov, A. I. *J. Am. Chem. Soc.* **1971**, *93*, 5620. (c) Greenberg, M. S.; Bodner, R. L.; Popov, A. I. *J. Phys. Chem.* **1973**, *77*, 2449.
(11) Ogata, T.; Fujisawa, T.; Tanaka, N.; Yokoi, H. *Bull. Chem. Soc. Jpn.* **1976**, *49*, 2759.
(12) Coetzee, J. F.; Karakatsanis, C. G. *Inorg. Chem.* **1976**, *15*, 3112.
(13) (a) Rusnak, L. L.; Yang, E. S.; Jordan, R. B. *Inorg. Chem.* **1978**, *17*, 1810. (b) Funahashi, S.; Jordan, R. B. *Inorg. Chem.* **1977**, *16*, 1301.

0020-1669/85/1324-1638$01.50/0